Lewis, W. K.; Gilliland, E. R. Glass Werner, Solid-catalyzed reaction in a fluidized bed. *AIChE J.* **1959**, *5* (4), 419.
McFatter, W. E.; Resen, F. L. Technical data of cat cracker Model 11. *Oil Gas J.* **1954**, *53* (21), 86.
McWhriter, W. E.; Tusson, J. R.; Parker, H. A. Detrehan Model 1V Fluid Cat Cracker. *Pet. Refin.* **1956**, *35* (4), 201.
May, W. G. Fluidized-bed reactor studies. *Chem. Eng. Prog.* **1959**, *55*, (12), 49.
Mathis, J. F.; Watson, C. C. Effect of fluidization on catalytic cumene dealkylation. *AIChE J.* **1956**, *2* (4), 518.
Mireur, J. P.; Bischoff, K. B. Mixing and contacting models for fluidized beds. *AIChE J.* **1967**, *13* (5), 839.
Reidel, J. C. Cities Serivce puts first Orthoflow cat cracker in United States on stream at Ponca City (Okla.). *Oil Gas J.* **1952** *50* (46), 200.
Resen, F. L. Model 1V cat cracker brings lower investment, plus more efficient operation to Pan-Am Southern at Detrehan. *Oil Gas J.* **1954a**, *52* (46), 214.
Resen, F. L. Suntide's new plant features vacuum unit, fluid cat cracker, HF alkylation and propylene tetramer unit, and unusual handling of segregated crudes. *Oil Gas J.* **1954b**, *52* (46), 203.
Resen, F. L. Operating report—nothing stands still at Suntide. Plant improvement started as first units went on stream. *Oil Gas J.* **1956**, *54* (42), 115.
Rowe, P. N. The effect of bubbles on gas–solids contacting in fluidized beds. *Chem. Eng. Prog., Symp. Ser.* **1962**, *58* (38), 42.
Shen, C. Y.; Johnstone, H. F. Gas–solids contact in fluidized beds. *AIChE J.* **1955**, *1* (3), 349.
Shnaider, G. S. Evaluation of the rate of reaction in single-stage and multistage reactors with fluidized beds. *Khim. Promst. (Moscow)*, **1966**, *6*, 35.
Shnaider, G. S. Some equations which describe catalytic cracking of oil fractions in fluidized beds of multistaged reactor. *Neftepererab. Neftekhim. (Moscow)* **1972a**, *12*, 9.
Shnaider, G. S. Grapho-analytical method of determination cetane numbers of light catalytic gas oils. *Khim. Tekhnol. Topl. Masel* **1972b**, *6*, 40.
Shnaider, G. S. Influence of catalyst-to-charge on the results of catalytic cracking of heavy distillates in multistaged reactor. *Khim. Tekhnol. Topl. Masel* **1973**, *1*, 12.
Shnaider, G. S. Evaluation of the Hydrodynamic Conditions in Multistaged Fluidized Countercurrent Flow Reactors in Pilot and Semicommercial Catalytic Cracking Units. *Chem. Eng. J.* **1988**, *38* (2), 97.
Shnaider, G. S.; Shnaider, A. G. Models of Catalytic Cracking of Oil Fractions in Single-stage and Multistage Reactors with Fluidized Beds and Interpretation of Experimental Data of Catalytic Cracking Performed in these Reactors. *Chem. Eng. J.* **1990**, in press.
Sittig, M. Catalytic Cracking Techniques in Review. *Pet. Refin.* **1952**, *31* (9), 263.
Spencer, H. A. A mixture of residue fraction and gas oil as feed for cat cracker Model 111. *Pet. Process.* **1954**, *9* (7), 1083.
Toei, R.; Matsuno, R.; Kojima, H.; Nagai, Y.; Nakagawa, K.; Yu, S. Behavior of bubbles in the gas–solid fluidized bed. *Chem. Eng. Jpn.* **1965**, *29*, 851.
Wheeler, H. K. New design features in catalytic cracker. *Pet. Eng.* **1951**, *23* (11), C-5.

Received for review April 4, 1989
Accepted June 11, 1990

PROCESS ENGINEERING AND DESIGN

Inadequacy of Steady-State Analysis for Feedback Control: Distillate–Bottom Control of Distillation Columns

Sigurd Skogestad* and Elling W. Jacobsen
Chemical Engineering, University of Trondheim (NTH), N-7034 Trondheim, Norway

Manfred Morari
Chemical Engineering 210-41, California Institute of Technology, Pasadena, California 91125

It is often claimed that for distillation columns the steady-state description is much more important than the dynamic description for control purposes. The ultimate counterexample to this misconseption is the recently proposed distillate–bottom (DB) configuration that involves using distillate and bottom flow to control compositions. This control scheme has previously been labeled "impossible" by most distillation control experts because D and B are not independent at steady state (since $D + B = F$) and the gain matrix is singular. Yet, as shown by Finco et al. for a propane–propylene splitter, both with simulations and with implementation, the scheme does actually work. Finco et al. do not provide any explanations for this, but as shown in this paper, the main reason is the flow dynamics (liquid lag from the top to the bottom of the column), which decouples the responses at high frequency (initial response) and makes the system quite easy to control. The results in this paper demonstrate that steady-state data may be entirely misleading for evaluating control performance. This is of course well-known, for example, from the Ziegler–Nichols tuning rules, which are based on high-frequency behavior only, but often seems to be forgotten when analyzing multivariable systems.

1. Introduction

The most important decision when designing distillation control systems is the selection of an appropriate control configuration. Finco et al. (1989) have recently proposed the distillate–bottom (DB) configuration, which involves using distillate and bottom flow to control compositions as a viable control scheme. An example of such a control scheme is shown in Figure 1. This control scheme has

0888-5885/90/2629-2339$02.50/0

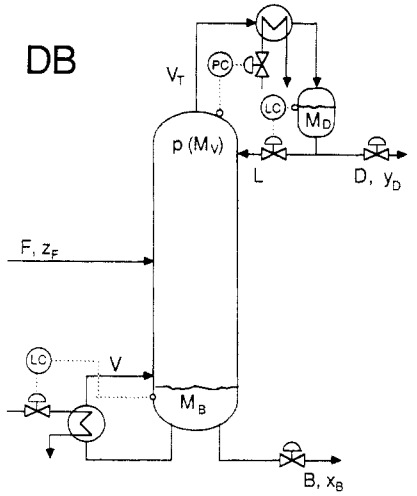

Figure 1. Two-product distillation column with DB configuration.

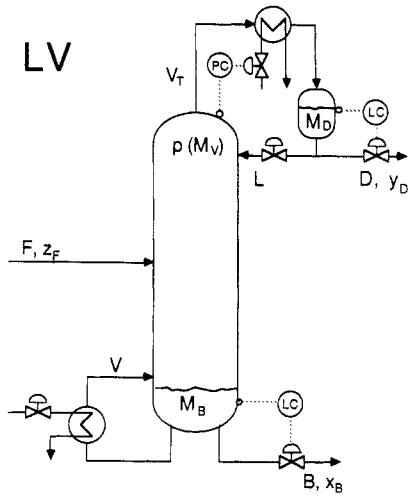

Figure 2. Two-product distillation column with LV configuration.

previously been labeled "impossible" or "nonoperable" by most distillation control experts (e.g., Perry and Chilton (1973, p 22–123), McCune and Gallier (1973), Shinskey (1984, p 154), Skogestad and Morari (1987c), Takamatsu et al. (1987), Häggblom and Waller (1988)). The only previous reference we have found that leaves the DB scheme some chance is by Waggoner (1983). He calls it "nonconventional" but says it may be implemented if it is accompanied with override control to protect the column. The main reason why the DB configuration has been rejected is that D and B are not independent at steady state because of the constraint $D + B = F$. In particular, the gain matrix is singular and the relative gain array (RGA) is infinite at steady state.

However, as shown by Finco et al. (1989) for a propane–propylene splitter, both with simulations and with implementation, the scheme does actually work. Imagine there is an increase in mole fraction of light component in the feed, z_F, to the column. To keep the top and bottom compositions constant, we know that the control system should increase D/F somewhat to maintain $Fz_F = Dy_D + Bx_B$, that is, $D/F = (z_F - x_B)/(y_D - x_B)$, and also adjust the internal flows (L and V) somewhat to maintain the overall separation. Assume the DB configuration is used for control. Initially following the increase in z_F, all flows are constant, but the bottom and top mole fractions, x_B and y_D, will start increasing slowly. As a response to the improved purity in the top, the control system will increase D, and as a response to the more impure bottom product, it will decrease B. This is exactly what the control system is supposed to do. But is the control system able to adjust the internal flows correctly? The answer is "yes"; the level control system will adjust L and V in response to changes in D and B made by the composition control system. Note that there are only 2 degrees of freedom at steady state. Consequently, if y_D and x_B are specified then there is only one possible solution for the flows D, B, L and V, and since the composition control system will keep changing D and B until the specifications are met, the internal flows will also be adjusted correctly.

However, the situation is actually not quite as simple as described above because the DB configuration would *not* work if there were no flow dynamics and the levels were controlled perfectly. The reason is that in this case the constaint $D + B = F$ would also apply dynamically and D and B could not be adjusted independently. Therefore, the DB configuration works only because it is possible to accumulate mass temporarily, which makes D and B independent variables from a dynamic point of view.

There are four possible sources of mass accumulation: reboiler holdup, condenser holdup, vapor holdup (pressure variations), and liquid holdup on the trays. Let $dL_T \equiv dL$ and dV_T represent small changes in the liquid and vapor flows in the top of the column, and let dL_B and $dV_B \equiv dV$ be changes in the bottom. The following relations between the flows apply dynamically (see Figure 1)

$$dL_T = c_D(s)(dV_T - dD) \tag{1}$$

$$dV_B = c_B(s)(dL_B - dB) \tag{2}$$

$$dV_T = c_p(s)\, dV_B \tag{3}$$

$$dL_B = g_L(s)\, dL_T \tag{4}$$

The first two equations assume that L_T and V_B are used for level control (DB configuration). The last two equations assume constant molar flows and neglect dynamic interactions between liquid and vapor flows; that is, vapor flow has no effect on liquid holdups. $c_D(s)$ and $c_B(s)$ are given by the level control systems, and $c_p(s)$ is primarily given by the pressure control system. The liquid lag from the top to the bottom of the column, $g_L(s)$, is a self-regulating effect given by the tray hydraulics. The overall liquid lag from the top to the bottom is assumed to be given by $\theta_L = N_{tr}\tau_L$ where $\tau_L = (\partial M_i/\partial L_i)_V$ is the hydraulic lag on each theoretical tray. With N_{tr} trays in series we get

$$g_L(s) = 1/\left(1 + \frac{\theta_L s}{N_{tr}}\right)^{N_{tr}} \tag{5}$$

In this paper, we shall use the above equations and furthermore assume $c_D(s) = c_B(s) = c_p(s) = 1$, that is, the trays are the only source of mass accumulation. The effect of not assuming perfect level and pressure control is briefly discussed toward the end.

The objective of this paper is to show why and for what columns the DB configuration works. We shall compare the DB scheme with the more conventional LV configuration shown in Figure 2.

Example Column. As an example column we shall use column D studied by Skogestad and Morari (1988a). This is a propane–propylene splitter similar to the one used by Finco et al. (1989), but we have assumed the relative volatility, α, to be constant throughout the column. Column data are given in Table I. We assume constant molar flows, negligible vapor holdup, and constant pressure. In this study we use $\theta_L = 1.54$ min. This is 20 times lower than the approximate 30 min used by Finco et al.

Table I. Data for Distillation Column Example[a]

z_F	α	N	N_F	$1 - y_D$	x_B	D/F	L/F
0.65	1.12	110	39	0.005	0.10	0.614	11.862

[a] Feed is liquid. Constant molar flows. Holdup on each theoretical tray, $M_i/F = 0.5$ min.

The industrial C3 splitters we have studied have had $\theta_L \approx 4$ min. Note that a change in holdup will simply scale all time constants, and therefore, these differences do not affect the conclusions in this paper. In a practical situation, larger holdups may be advantageous—at least for disturbance rejection—because the effect of analyzer dead times is less important.

2. Modeling

Detailed modeling of the column including flow dynamics yields a set of differential equations with two states for each tray. Typically these states are chosen to be the mole fraction of one component and the holdup. Because of the large number of trays, the full-order model for the example column has 222 states. This makes numerical calculations extremely time consuming. Because of this and to make the exposition clearer, we choose to use a simple low-order model for the column.

Derivation of Model for DB Configuration from LV Configuration. It may be difficult to formulate directly a simple model for the DB configuration because the steady-state gains are infinite. A better approach is to start with a model for a base configuration and subsequently use flow relationships to derive a model for the DB configuration. The LV scheme is preferred as the base configuration because the composition dynamics for the LV configuration are only weakly dependent on the reboiler and condenser holdups (and on the tuning of the level loops). Write the linear model for the LV scheme as

$$\begin{pmatrix} dy_D \\ dx_B \end{pmatrix} = G^{LV}(s) \begin{pmatrix} dL \\ dV \end{pmatrix} \tag{6}$$

Assume the flows are independent of compositions. Then simple flow relationships such as (1)–(4) above may be used to eliminate dL_B and dV_T and express dL and dV as functions of the independent variables dD and dB:

$$\begin{pmatrix} dL \\ dV \end{pmatrix} = M_{LV}^{DB}(s) \begin{pmatrix} dD \\ dB \end{pmatrix} \tag{7}$$

The linear model for the DB configuration

$$\begin{pmatrix} dy_D \\ dx_B \end{pmatrix} = G^{DB}(s) \begin{pmatrix} dD \\ dB \end{pmatrix} \tag{8}$$

becomes

$$G^{DB}(s) = G^{LV}(s) M_{LV}^{DB}(s) \tag{9}$$

Assume perfect level and pressure control for the DB configuration; i.e., $c_D = c_B = c_p = 1$. Then (1)–(4) yield $dV = g_L(s)\, dL - dB$ and $dL = dV - dD$. Thus, we obtain

$$M_{LV}^{DB}(s) = \frac{1}{1 - g_L(s)} \begin{pmatrix} -1 & -1 \\ -g_L(s) & -1 \end{pmatrix} \tag{10}$$

Simple Two-Time-Constant Model. We choose to use the simple two-time-constant model presented by Skogestad and Morari (1988a). This model was derived assuming the flow and composition dynamics to be decoupled. In reality, the flow dynamics do affect the composition dynamics, and the model may be somewhat in error. In particular, the time constant τ_2 may be larger than that given by Skogestad and Morari (1988a). However, as we shall see, the final results derived in this paper do not depend on τ_2.

Table II. Data Used in the Simple Model of the Distillation Column

steady-state gains (scaled compositions, eq 15)

$$G^{LV}(0) = \begin{pmatrix} 24.585 & -24.2 \\ 21.270 & -21.3 \end{pmatrix}$$

time contants $\tau_1 = 154$ min; $\tau_2 = 30$ min; $\theta_L = 1.54$ min

The simple two-time-constant model of the LV configuration including liquid flow dynamics is

$$G^{LV}(s) = \begin{pmatrix} \dfrac{k_{11}}{1 + \tau_1 s} & \dfrac{k_{11} + k_{12}}{1 + \tau_2 s} - \dfrac{k_{11}}{1 + \tau_1 s} \\ \dfrac{k_{21}}{1 + \tau_1 s} g_L(s) & \dfrac{k_{21} + k_{22}}{1 + \tau_2 s} - \dfrac{k_{21}}{1 + \tau_1 s} \end{pmatrix} \tag{11}$$

where $k_{ij} = g_{ij}^{LV}(0)$ denote the steady-state gains for the LV configuration.

By using (9) and (10), the simplified model of the DB configuration becomes

$$G^{DB}(s) = \begin{pmatrix} \dfrac{k_{11}}{1 + \tau_1 s} + \dfrac{g_L(s)}{1 - g_L(s)} \dfrac{k_{11} + k_{12}}{1 + \tau_2 s} & \dfrac{1}{1 - g_L(s)} \dfrac{k_{11} + k_{12}}{1 + \tau_2 s} \\ \dfrac{g_L(s)}{1 - g_L(s)} \dfrac{k_{21} + k_{22}}{1 + \tau_2 s} & \dfrac{k_{21}}{1 + \tau_1 s} + \dfrac{1}{1 - g_L(s)} \dfrac{k_{21} + k_{22}}{1 + \tau_2 s} \end{pmatrix} \tag{12}$$

Note that the model is written in terms of the steady-state gains k_{ij} of the LV configuration. The steady-state gains for the DB configuration are infinite in magnitude as seen from the low-frequency approximations

$$\lim_{s \to 0} g_L(s) = 1; \quad \lim_{s \to 0} \frac{1}{1 - g_L(s)} = \frac{1}{N\tau_L s} = \frac{1}{\theta_L s} \tag{13}$$

and

$$\lim_{s \to 0} G^{DB}(s) = -\frac{1}{\theta_L s} \begin{pmatrix} k_{11} + k_{12} & k_{11} + k_{12} \\ k_{21} + k_{22} & k_{21} + k_{22} \end{pmatrix} \tag{14}$$

The physical interpretation is that a decrease in, for example, D with B constant will immediately yield a corresponding increase in L. This increase will yield a corresponding increase in V, which subsequently will increase L even more, etc. Consequently, the effect is that the internal flows eventually will approach infinity. Mathematically, there is an integrator at low frequency: As $s \to 0$ we have $dL = dV = -(dD + dB)/\theta_L s$.

Also note that the steady-state gain matrix of the DB configuration is singular. One might expect that this implies control problems, but this turns out not to be the case.

Example Column. Data for the simple models described above are given in Table II. The gain data in Table II are for scaled (logarithmic) compositions

$$\Delta y_D^s = \Delta y_D/(1 - y_D) = \Delta y_D/0.005$$
$$\Delta x_B^s = \Delta x_B/x_B = \Delta x_B/0.10 \tag{15}$$

The flow dynamics are given by

$$g_L(s) = 1/(1 + (1.54/n)s)^n \tag{16}$$

To reduce the order, we used $n = 5$ instead of the actual $N_{tr} = 109$. The magnitude of the transfer matrix elements in LV and DB configurations are plotted as a function of

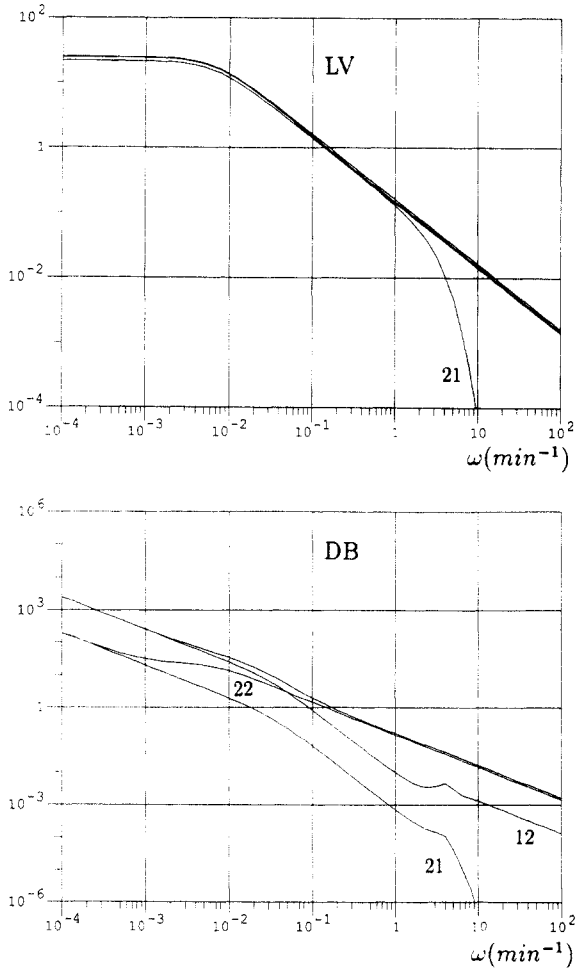

Figure 3. Gain elements $|g_{ij}|$ as a function of frequency for LV and DB configurations.

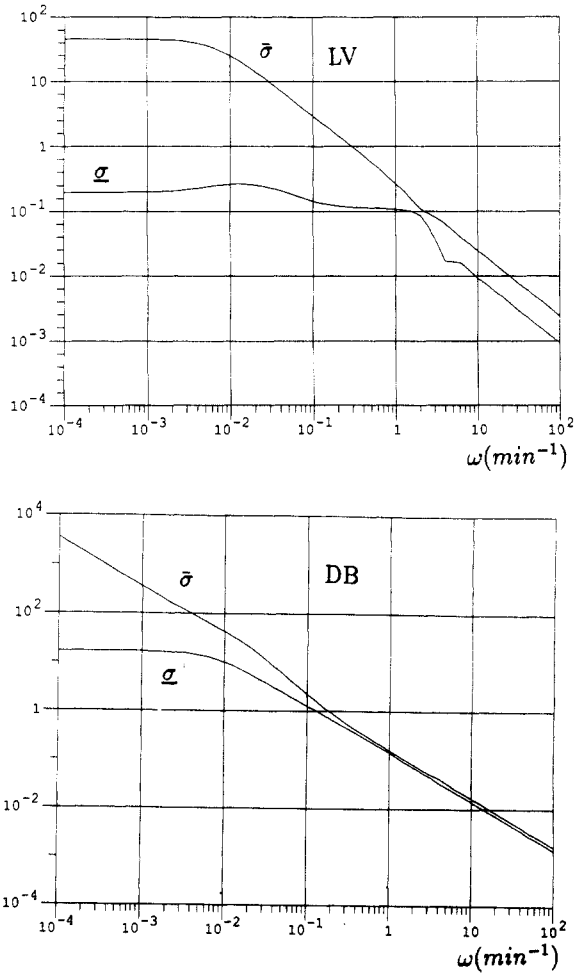

Figure 4. Singular values as a function of frequency for LV and DB configurations.

frequency in Figure 3. Note that the flow dynamics make the plant models triangular at high frequency.

3. Analysis of the Model

Poles and Zeros at $s = 0$. As noted above, the gain matrix for the DB configuration is singular at steady state; that is, $G^{DB}(s)$ must have a zero at $s = 0$. Furthermore, the steady-state gain is infinite in one direction (corresponding to the largest singular value); that is, $G^{DB}(s)$ must have a pole at $s = 0$. To study this in more detail, consider eq 12. It is easily shown that this model has two poles at $s = 0$ and one transmission zero at $s = 0$. The zero at $s = 0$ corresponds to the direction $dD = -dB$. However, physically we know that this change has a finite and not zero gain at steady state, and the zero must therefore correspond to a pole–zero cancellation in the process. This is also clear as we may easily show that there exists physical realizations with only one pole at $s = 0$. No signals may enter between the zero and pole, which implies that there will be no problem with internal stability.

Singular Values and Relative Gain Array. Singular values and the 1,1 element of the RGA (simply denoted λ in the following) for the simplified models are shown as a function of frequency in Figure 4 and Figure 5. Note the singular values for the DB configuration. As expected, at low frequency the maximum singular value (maximum gain corresponding to change in internal flows) behaves like an integrator and approaches infinity. It may seem somewhat puzzling that the gain matrix of the DB configuration approaches singularity at low frequencies even though the minimum singular value is non-zero at steady

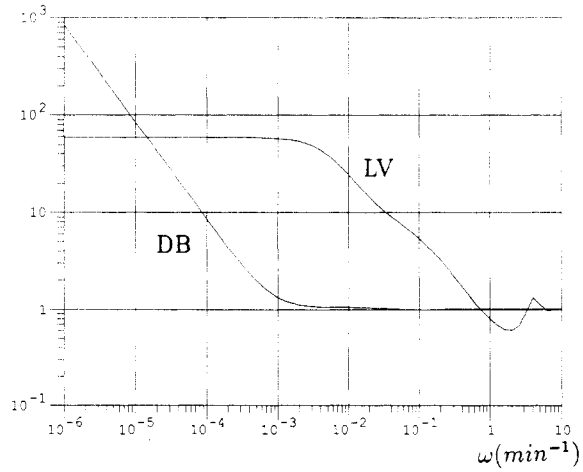

Figure 5. $|\lambda|$ as a function of frequency for LV and DB configurations.

state. However, note that the maximum singular value approaches infinity such that the ratio between the two singular values is infinity.

Usually, only the steady-state value of the RGA is considered (e.g., Shinskey, 1984; Grosdidier et al., 1985). However, it has been suggested that the frequency-dependent RGA may yield additional information (e.g., McAvoy, 1983), and newer results support this. Skogestad and Morari (1987b) show that large RGA values indicate a plant that is very sensitive to element-by-element uncertainty and, even more importantly, to input uncertainty,

and single-loop controllers should be used. Nett (1987) has demonstrated that RGA values close to 1 at frequencies corresponding to the closed-loop bandwidth imply that single-loop controllers may be designed independently. For our example, a reasonable closed-loop bandwidth is about 0.1 min^{-1}. As one measure of how easy a configuration is to control, we shall consider the frequency, ω_1, where the RGA approaches one.

The RGA element λ for the LV configuration starts out at a steady state value of 59 and then falls off with a −1 slope on the log–log plot and crosses one at the frequency $\omega_1 \approx 1/\theta_L = 0.6$ min^{-1}. λ for the DB configuration is infinite at steady state. It falls off with a −1 slope, and the low-frequency asymptote crosses one at $\omega_1 \approx 0.001$ min^{-1}. Thus, although the RGA for the DB configuration is much worse (higher) than for the LV configuration at low frequency, it is significantly better (closer to one) in the frequency range important for feedback control, that is, in the frequency range from about 0.01 to 1 min^{-1}. The observation of Finco et al. (1989) that the DB configuration gave better control performance than the LV configuration is therefore not surprising from the RGA values. In fact, from the RGA values, the column seems to be quite simple to control by using the DB configuration.

Analytical Treatment of RGA. The 1,1 element of the RGA is defined as

$$\lambda(s) = \left(1 - \frac{g_{12}(s)g_{21}(s)}{g_{11}(s)g_{22}(s)}\right)^{-1} \tag{17}$$

We shall use the simple two-time-constant model to derive analytical expressions for the frequency, ω_1, where $|\lambda|$ approaches one.

LV Configuration. For the LV configuration, it is easily shown that this is at about

$$\omega_1^{LV} = 1/\theta_L \tag{18}$$

for all columns. This is not surprising since $1/\theta_L$ is the frequency at which the system becomes decoupled (recall Figure 3).

DB Configuration. From Figure 5, we see that ω_1^{DB} may be obtained as the frequency where the low-frequency asymptote of $|\lambda^{DB}(\omega)|$ crosses one. The same holds for a number of other example columns (Skogestad et al., 1990). Consider the simple model (12) and introduce the steady-state gains k_{ij}^{DV} for the DV configuration: For constant molar flows and perfect control of condenser level, we have $dL = dV - dD$ and $k_{11}^{DV} = -k_{11}^{LV}$, $k_{12}^{DV} = k_{11}^{LV} + k_{12}^{LV}$, $k_{21}^{DV} = -k_{21}^{LV}$, and $k_{22}^{DV} = k_{21}^{LV} + k_{22}^{LV}$. We get

$$G^{DB}(s) = \begin{pmatrix} \dfrac{-k_{11}^{DV}}{1+\tau_1 s} + \dfrac{g_L(s)}{1-g_L(s)}\dfrac{k_{12}^{DV}}{1+\tau_2 s} & \dfrac{1}{1-g_L(s)}\dfrac{k_{12}^{DV}}{1+\tau_2 s} \\ \dfrac{g_L(s)}{1-g_L(s)}\dfrac{k_{22}^{DV}}{1+\tau_2 s} & \dfrac{-k_{21}^{DV}}{1+\tau_1 s} + \dfrac{1}{1-g_L(s)}\dfrac{k_{22}^{DV}}{1+\tau_2 s} \end{pmatrix} \tag{19}$$

Consider low frequencies where $(1+\tau_2 s)/(1+\tau_1 s) \approx 1$ and derive from (19)

$$\lambda^{DB}(s) = \frac{([g_L(s)k_{12}^{DV} - (1-g_L(s))k_{11}^{DV}][k_{22}^{DV} + (1-g_L(s))k_{21}^{DV}])}{((1-g_L(s))[g_L(s)k_{12}^{DV}\,k_{21}^{DV} - k_{11}^{DV}\,k_{22}^{DV} - (1-g_L(s))k_{11}^{DV}\,k_{21}^{DV}])} \tag{20}$$

The low-frequency asymptote ($s \to 0$) is (recall eq 13)

$$\lambda^{DB}(s \to 0) = \lambda^{DV}(0)\frac{-k_{12}^{DV}}{k_{11}^{DV}}\frac{1}{\theta_L s} \tag{21}$$

Here we have for constant molar flows and for binary columns with reasonably high purity (Skogestad and Morari, 1987a)

$$\lambda^{DV}(0) \approx 1/\left(1 + \frac{Bx_B}{D(1-y_D)}\right) \tag{22}$$

$$-\frac{k_{12}^{DV}}{k_{11}^{DV}} = -\frac{(\partial y_D/\partial V)_D}{(\partial y_D/\partial D)_V} \approx Bx_B\left(\frac{\partial \ln S}{\partial V}\right)_D \tag{23}$$

where S is the separation factor. This yields the following approximation:

$$\omega_1^{DB} = \frac{1}{\dfrac{1}{Bx_B} + \dfrac{1}{D(1-y_D)}}\left(\frac{\partial \ln S}{\partial V}\right)_D \frac{1}{\theta_L} \tag{24}$$

To evaluate this expression further, we need to know how the separation factor depends on changes in internal flows. The approximate column model

$$S = \alpha^N \frac{(L/V)_T^{N_T}}{(L/V)_B^{N_B}} \tag{25}$$

with $N_T = N_B = N/2$ yields for liquid feeds (Skogestad and Morari, 1987a)

$$\left(\frac{\partial \ln S}{\partial V}\right)_D \approx \frac{N}{2(L/F)L_B} \tag{26}$$

Skogestad and Morari (1987a) found (26) to be reasonably accurate for most columns. For well-designed columns with liquid feed and relative volatility less than about 2, we have (Skogestad and Morari, 1988a)

$$\frac{N}{2} \approx N_{min} = \frac{\ln S}{\ln \alpha} \approx \frac{\ln S}{\alpha - 1} \approx (L/F)\ln S \tag{27}$$

and we have $(\partial \ln S/\partial V)_D \approx \ln S/L_B$ where $\ln S$ is in the range 4–10 for most columns. Substituting into (24) yields

$$\omega_1^{DB} \approx \frac{1}{\left[\dfrac{1}{Bx_B} + \dfrac{1}{D(1-yD)}\right]}\frac{\ln S}{L_B}\omega_1^{LV} \tag{28}$$

The term multiplying ω_1^{LV} is much less than one for high-purity columns and for columns with large reflux. Thus, although the RGA for the DB configuration is much worse (higher) than for the LV configuration at low frequency, it is significantly better (closer to one) in the frequency range important for feedback control, that is, in the frequency range from about 0.01 to 1 min^{-1}.

Example Column. For the example column, (26) gives $(\partial \ln S/\partial V)_D = 0.46$ (the exact value is 0.36) and we derive from (24) that $\omega_1^{DB} = 0.0028(0.46/\theta_L) = 0.0013/\theta_L = 0.0009$ min^{-1}. This is very close to the observed value of 0.001 min^{-1} in Figure 5. Equation 28 also gives the same value.

Disturbance Rejection. The main reason for applying feedback to distillation columns is to counteract the effect of disturbances. The RGA says nothing about disturbances. The most important disturbances are feed composition, feed flow, reflux flow, and boilup.

To evaluate the effect of disturbances, consider the "open-loop" model, that is, with the two variables for composition control kept constant. For disturbances in reflux and boilup, the effect on compositions is zero for the DB configuration if level control is assumed perfect. For the LV configuration, it is given by the open-loop gains in Figure 3. For disturbances in feed composition, there is no difference between the configurations if we assume constant molar flows such that compositions do not affect

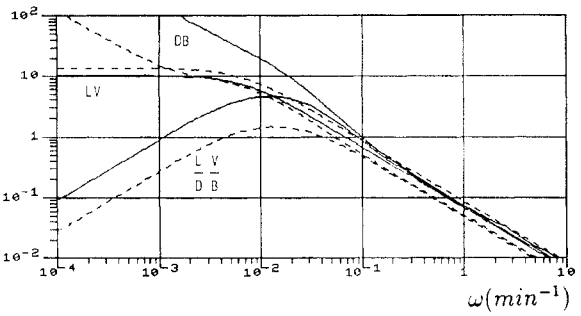

Figure 6. Effect of disturbances in F on compositions using three different configurations: LV, DB, and $(L/D)(V/B)$. Solid line: $(\delta y_D^s/\delta F)$. Dotted line: $(\delta x_B^s/\delta F)$.

Table III. PI Settings Used in Simulations: $c(s) = k[(1 + \tau_I s)/\tau_I s]$. Gains k_y and k_x Are for Scaled Compositions (Equation 15)

configuration	τ_{Iy}, min	τ_{Ix}, min	k_y	k_x
LV	7.38	4.00	1.76	0.96
DB	5.89	4.35	3.53	2.61

flows. For disturbances in feed rate, the DB configuration is more sensitive than the LV configuration, at least at low frequency. In Figure 6, the gain for the effect of a feed flow disturbance on compositions is diplayed as a function of frequency. At steady state, the effect of this disturbance on compositions is infinite for the DB configuration. However, the difference between the LV and DB configurations is quite small at high frequencies. For comparison Figure 6 also shows the feed disturbance gain for the $(L/D)(V/B)$ configuration. Even though this configuration is insensitive at steady state, the initial response is similar to that of the other configurations.

In summary, the DB configuration is also better than the LV configuration when disturbances are taken into account (because it is insensitive to disturbances in reflux and boilup). However, it is probably not quite as good as the $(L/D)(V/B)$ configuration.

Simulations. Simulations of the LV and DB configurations with a full-order nonlinear model with 222 states are shown in Figure 7. The PI controllers C in Table III were obtained from the simplified models G as follows: Maximize the ratio k/τ_I such that the worst-case (with model error as defined by Skogestad and Morari (1988b)) peak of $\bar{\sigma}((I + GC(j\omega))^{-1})$ is less than 2. This maximizes the controller gain at low and intermediate frequencies for good performance, but guarantees a reasonable robustness margin. For simplicity, k/τ_I was assumed equal in the two loops. The simulation results are similar to the ones obtained by Finco et al. and confirm that the DB configuration is better for two-point control than the LV configuration. We note in particular that the DB configuration shows much less interaction than the LV configuration.

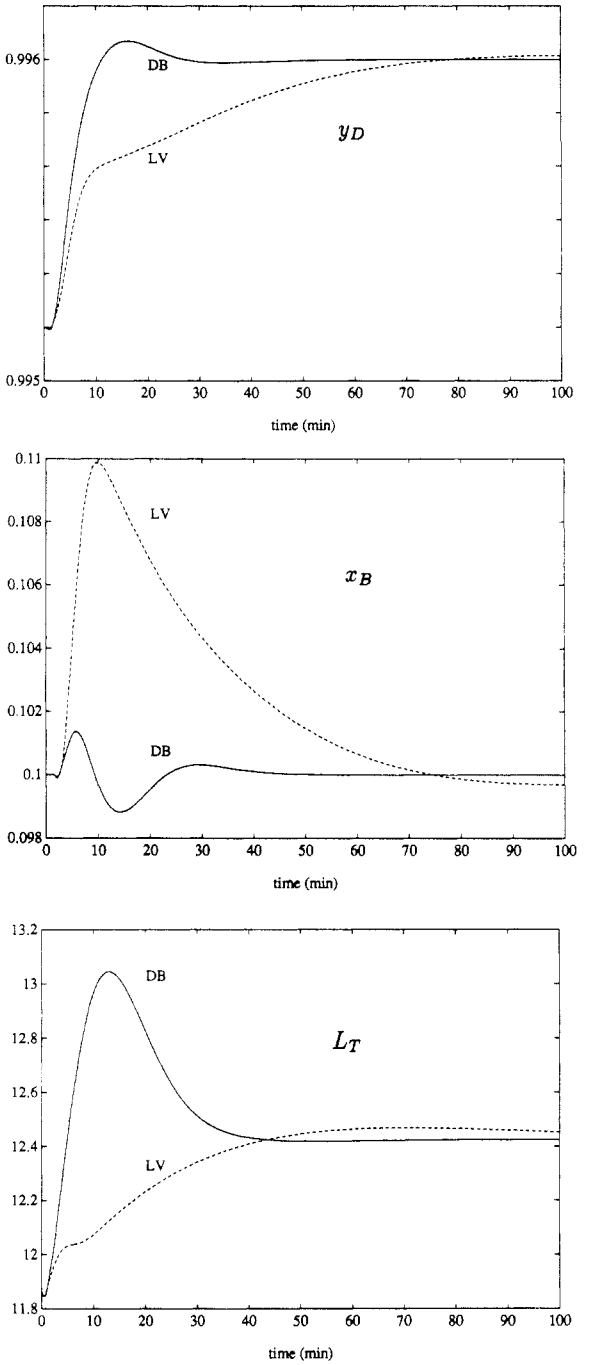

Figure 7. Time responses of y_D, x_B, and L to a setpoint change $\Delta y_D = 0.001/(5s + 1)$ for the LV and DB configurations. A time delay of 1 min in each loop is included.

4. Discussion

The analytical results presented in this paper are based on simplified linear models such as eq 12. However, we have found that the use of a full-order linear model (with $2N + 2$ states) yields very similar results. Furthermore, the simulations confirm that the linear analysis holds also in the nonlinear case.

The results were also derived assuming perfect control of level and pressure. With regard to interactions as measured in terms of the RGA, these will become less for the DB configuration when levels and pressure are not perfectly controlled. The reason is that the time for the mass to recycle within the column is increased and D and B become more independent. With perfect level control, this recycle time is about θ_L. Now, assume the transfer functions for pressure and level control are given by

$$c_D(s) = \frac{1}{1 + \tau_D s}; \quad c_B(s) = \frac{1}{1 + \tau_B s}; \quad c_p(s) = \frac{1}{1 + \tau_p s} \tag{29}$$

(These simple transfer functions will be obtained with pure proportional controllers). In this case, the total time for mass to recycle is about $\theta_r = \theta_L + \tau_D + \tau_B + \tau_p$, and it is probably not too surprising that the results in terms of the low-frequency asymptotes of the RGA for the DB configuration given above, e.g., eq 24, are unchanged but with θ_L replaced by θ_r. Note that although the DB configuration

is improved with respect to *interactions* by introducing lags τ_D and τ_B, the overall control performance may be worse because changes in D and B will not immediately affect L and V. This may be partially counteracted by applying "feedforward" action from D to L and from B to V; that is, set $dL = -dD$ and $dV = -dB$. This is equivalent to letting the level controllers set $L + D$ and $V + B$ rather than L and V. The LV configuration is generally insensitive to level dynamics, and the introduction of lags τ_D and τ_B has almost no effect on RGA or control performance.

The DB configuration has previously been labeled "impossible" because the inputs D and B are not independent at steady state. This conclusion is partly correct for one-point composition control, but we have shown that for two-point control the DB configuration is actually quite easy to control at high frequency and will perform better than the LV configuration for most columns, in particular for columns with high-purity products and/or large reflux.

However, as pointed out by Finco et al. (1989), the DB configuration lacks integrity, as it will not work satisfactorily if one of the inputs D or B for some reason is no longer used for feedback control. The reason is that this will lock the product split D/B, and good control of either composition is impossible. Since most industrial columns are operated with one-point composition control (that is, one input in manual), this is probably the reason why the DB configuration has not been applied in industry, and it is also the reason why industrial practicioners have advised against it (e.g., McCune and Gallier, 1973). The integrity problems may be handled by use of an override control scheme (Finco et al., 1989).

One alternative to the DB configuration for two-point control is the $(L/D)(V/B)$ configuration, which, in addition, is good for one-point control. However, it requires all flows L, D, V and B to be measured or estimated, which makes implementation more difficult. The main advantage of the DB configuration is that it is very easy to implement. This advantage has to be weighed against its lack of integrity.

5. Conclusion

As one measure of how easy a column is to control, we considered the frequency, ω_1, where the magnitude of the 1,1 element of the RGA, $|\lambda(j\omega)|$, approaches one. For the LV configuration, this is at about $\omega_1^{LV} = 1/\theta_L$, where θ_L is the overall liquid lag from the condenser to the reboiler. For the DB configuration, the RGA is infinite at low frequency but decreases with a -1 slope on a log–log plot. Analytical approximations for the case with perfect level and pressure control yield

$$\omega_1^{DB} \approx \frac{1}{1/Bx_B + 1/D(1 - y_D)} \frac{\ln S}{L_B} \omega_1^{LV}$$

where S is the separation factor. The term multiplying ω_1^{LV} is much less than one for high-purity columns and for columns with large reflux. Thus, although the RGA for the DB configuration is much worse (higher) than for the LV configuration at low frequency, it is significantly better (closer to one) in the frequency range important for feedback control, that is, in the frequency range from about 0.01 to 1 min^{-1}.

The control behavior of the DB configuration is therefore an excellent example of how misleading steady-state arguments may be for evaluating control performance. For feedback control, the plant behavior in the frequency region corresponding to the closed-loop bandwidth is of primary importance, and the steady state is useful only if it reflects this behavior. This is, of course, well-known, for example from the Ziegler–Nichols tuning rules, which are based on high-frequency behavior only, but it often seems to be forgotten when analyzing multivariable systems.

Acknowledgment

This work was made possible by financial support from NTNF and NSF.

Nomenclature

$G(s)$ = model for effect of flows on compositions
$k_{ij} = g_{ij}^{LV}(0)$ = steady-state gains for the LV configuration
$L \equiv L_T$ = reflux flow rate (kmol/min)
L_B = liquid flow rate into reboiler (kmol/min)
M_i = liquid holdup on theoretical tray i (kmol)
N = number of theoretical stages in column (including reboiler)
$N_{tr} = N - 1$ = number of trays in column
N_T = number of theoretical stages in rectifying section
N_B = number of theoretical stages in stripping section
RGA = Relative Gain Array, elements are λ_{ij}
$S = [y_D(1 - x_B)]/[(1 - y_D)x_B]$ = separation factor
$V \equiv V_B$ = boilup from reboiler (kmol/min)
V_T = vapor flow rate on top tray (kmol/min)
x_B = mole fraction of light component in bottom product
y_D = mole fraction of light component in distillate (top product)
z_F = mole fraction of light component in feed

Greek Symbols

$\alpha = (y_i/x_i)/[(1 - y_i)/(1 - x_i)]$ = relative volatility
$\lambda(s) = (1 - [g_{12}(s)g_{21}(s)]/[g_{11}(s)g_{22}(s)])^{-1}$ = 1,1 element in RGA
ω = frequency (min^{-1})
ω_1 = frequency where $|\lambda(j\omega_1)|$ approaches 1.
$\bar{\sigma}(G), \underline{\sigma}(G)$ = maximum and minimum singular values
τ_1 = dominant time constant for external flows (min)
τ_2 = time constant for internal flows (min)
τ_L = hydraulic lag on each theoretical tray (min)
$\theta_L = N_{tr}\tau_L$ = overall lag for liquid response (min)
θ_r = overall lag including level and pressure control (min)

Literature Cited

Finco, M. V.; Luyben, W. L.; Polleck, R. E. Control of Distillation Columns with Low Relative Volatility. *Ind. Eng. Chem. Res.* **1989**, *28*, 76–83.

Grosdidier, P.; Morari, M.; Holt, B. R. Closed-Loop Properties from Steady State Gain Information. *Ind. Eng. Chem. Fundam.* **1985**, *24*, 221–235.

Häggblom, K. E.; Waller, K. V. Transformations and consistency relations of distillation control structures. *AIChE J.* **1988**, *34* (10), 1634–1648.

McAvoy, T. J. *Interaction Analysis*; Instrument Society of America: Research Triangle Park, NC, 1983.

McCune, L. C.; Gallier, P. W. Digital Simulation: A Tool for the Analysis and Design of Distillation Control. *ISA Trans.* **1973**, *12* (3), 193–207.

Nett, C. N. Presented at the American Control Conference, Minneapolis, MN, June 1987.

Perry, H. P., Chilton, C. H., Eds. *Chemical Engineers's Handbook*, 5th ed.; McGraw-Hill: New York, 1973.

Shinskey, F. G. *Distillation Control*, 2nd ed.; McGraw-Hill: New York, 1984.

Skogestad, S.; Morari, M. A Systematic Approach to Distillation Column Control. Distillation 87, Brighton; *Inst. Chem. Eng. Symp. Ser.* **1987a**, *104*, A71–A86.

Skogestad, S.; Morari, M. Implication of Large RGA-Elements on Control Performance. *Ind. Eng. Chem. Res* **1987b**, *26*, 2121–2330.

Skogestad, S.; Morari, M. Control Configuration Selection for Distillation Columns. *AIChE J.* **1987c**, *33* (10), 1620–1635.

Skogestad, S.; Morari, M. Understanding the Dynamic Behavior of Distillation Columns. *Ind. Eng. Chem. Res.* **1988a**, *27*, 1848–1862.

Skogestad, S.; Morari, M. LV-Control of a High-Purity Distillation Column. *Chem. Eng. Sci.* **1988b**, *43* (1), 33-48.
Skogestad, S.; Lundström, P.; Jacobsen, E. W. Selecting the best distillation control configuration. *AIChE J.* **1990**, *36* (5), 753-764.
Takamatsu, T.; Hashimoto, I.; Hashimoto, Y. Selection of manipulated variables to minimize interaction in multivariate control of distillation column. *Inst. Chem. Eng.* **1987**, *27* (4), 669-677.
Waggoner, R. C. Distillation Column Control. *AIChE Modular Instruction. Series A: Process Control*; AIChE: New York, 1983; Vol. A5, pp 19-29.

Received for review May 5, 1989
Revised manuscript received May 23, 1990
Accepted June 1, 1990

SEPARATIONS

Changes in Particle Morphology during Drying of Drops of Carbohydrate Solutions and Food Liquids. 1. Effects of Composition and Drying Conditions

Tarric M. El-Sayed,[†] David A. Wallack,[‡] and C. Judson King*
Department of Chemical Engineering, University of California, Berkeley, California 94720

Morphological changes of drops of sucrose and maltodextrin solutions, coffee extract, and skim milk have been monitored during drying. One method involved videotaping drops suspended in a stream of hot air. A second method was to sample a stream of drops of uniform initial size falling through a column with a controlled temperature profile. Suspended drops show a first period of near-spherical shrinkage, closely following predictions for a voidless sphere. This is followed by a second period of rapid inflate–deflate cycling (boiling) and a third and final period during which the drop grows and/or shrinks to reach a solidified morphology. The effects of composition, air temperature, initial solute concentration, and presence or absence of dissolved gases were determined. Particles of coffee extract from the falling-drop dryer evidence surface blowholes, replicating what is observed in commercial spray-dried coffee. This phenomenon is rationalized in terms of viscous resistance to sealing flows.

Introduction

Drops of liquid solutions undergo changes in morphology—size, shape, and appearance—as they dry evaporatively to form solid particles. In most cases, an initially spherical liquid drop does not simply become a solid, spherical particle. Appearances of typical particles from a commercial instant-coffee spray dryer are shown in Figure 1. Particles develop internal voidage and surface irregularities (folds, blowholes, etc.). They also expand, collapse, and/or shrivel. These phenomena are not limited to spray drying. For example, similar morphologies have been found for fly-ash particles (Fisher et al., 1976).

In spray drying, changes in particle morphology during drying govern the bulk density of the product and should affect drying rates (see part 2) and ease of redissolution. For spray drying of a food product, certain morphological changes, e.g., surface ruptures, probably cause substantial losses of volatile flavor and aroma components.

The goal of the present research was to gain further insight into how the nature of the material being dried and the drying conditions govern the development of particle morphology. Two experimental approaches were used. In one, drops suspended from a glass fiber or a thermocouple were dried in a stream of hot air. The appearances of the drops during drying were recorded continuously by video photography onto videotape for subsequent playback. In the second method, a stream of drops of initially uniform size fell through a vertical column with a known, predetermined temperature field. Samples obtained at various levels along the fall were frozen in situ, freeze dried, and observed by scanning electron microscopy. Drops were formed from aqueous solutions of sucrose, maltodextrin, coffee extract, and skim milk, chosen so as to display different types of morphological features.

Previous Work. Microscopic observation is useful for examining the particle morphology of a dried product but does not give direct information on how the final morphology came about.

One technique that has been used for monitoring changes in particle morphology continually during drying has been observation of stationary, suspended macrodrops, typically 1–5 mm in diameter. Charlesworth and Marshall (1960) reported differences in morphological development during drying of suspended drops of various salts and coffee extract. Similar experiments were carried out by Abdul-Rahman et al. (1971) and Crosby and Weyl (1977).

Artifacts are introduced into suspended-drop experiments by the suspension device, the lack of free rotation, and the relatively large drop size. Alternative approaches are experimentally more complicated. Toei and co-workers

* To whom correspondence should be addressed.
[†] Present address: Clorox Corporation, Technical Center, Pleasanton, CA 94566.
[‡] Present address: 3M Corporation, St. Paul, MN 55119.

0888-5885/90/2629-2346$02.50/0